

Supporting information

Conductive Framework Embedded with Cobalt doped Vanadium Nitride as Efficient Polysulfide Adsorber and Convertor for Advanced Lithium-sulfur Batteries

Yang Lu,^{*#a} Menglong Zhao,^{#a} Ya Yang,^a Mengjie Zhang,^a Ning Zhang,^a Hailong Yan,^a Tao Peng,^a Xianming Liu,^b and Yongsong Luo^{*ac}

^aHenan Joint International Research Laboratory of New Energy Storage Technology, Key Laboratory of Microelectronics and Energy of Henan Province, School of Physics and Electronic Engineering, Xinyang Normal University, Xinyang 464000, P. R. China.

^bCollege of Chemistry and Chemical Engineering, Luoyang Normal University, Luoyang 471934, P. R. China.

^cCollege of Physics and Electronic Engineering, Nanyang Normal University, Nanyang 473061, P. R. China.

*Corresponding author. Tel./fax: +86 376 6390801, E-mail: luyang.181@163.com (Y. Lu), ysluo@xynu.edu.cn (Y. S. Luo).

#Yang Lu and Menglong Zhao contributed equally to this work.

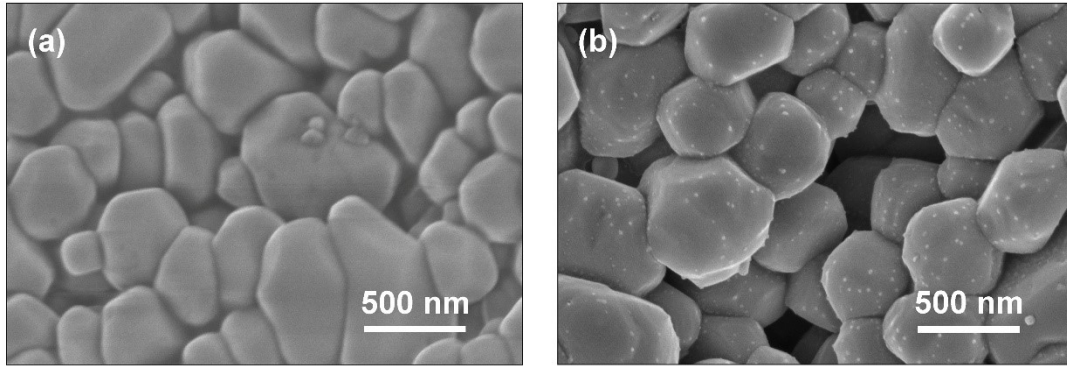


Figure S1. (a) SEM images of the NaCl@Co-V precursor after freeze-drying. (b) SEM images of Co-VN/NC before removal of the NaCl template.

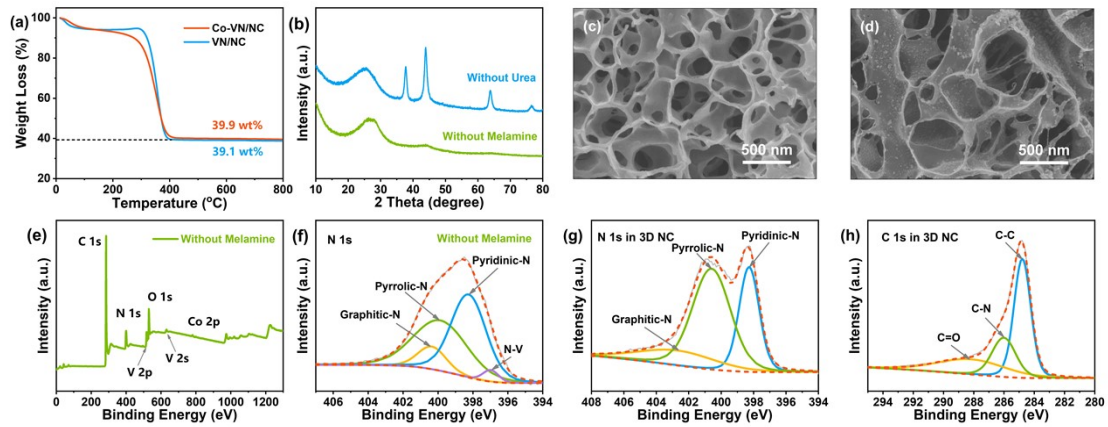


Figure S2. (a) the thermogravimetric analysis of Co-VN/NC in Air. (b) XRD pattern of the samples in control experiments. (c) SEM images of the sample were annealed without adding melamine. (d) SEM images of Co-VN/NC without adding urea. (e, f) The full XPS survey spectrum and high-resolution spectra of the sample without melamine, respectively. (g, h) High-resolution XPS spectra of N 1s and C 1s in 3D NC, respectively.

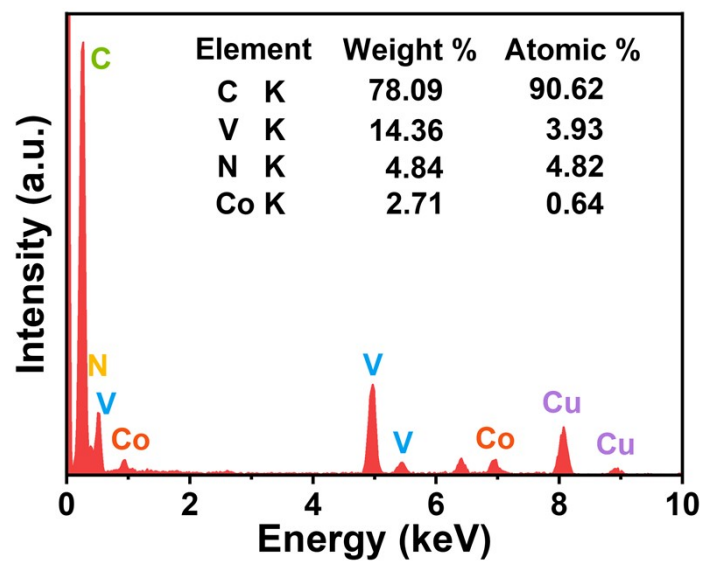


Figure S3. The EDX spectrum of Co-VN/NC, where the Cu signals come from the copper mesh.

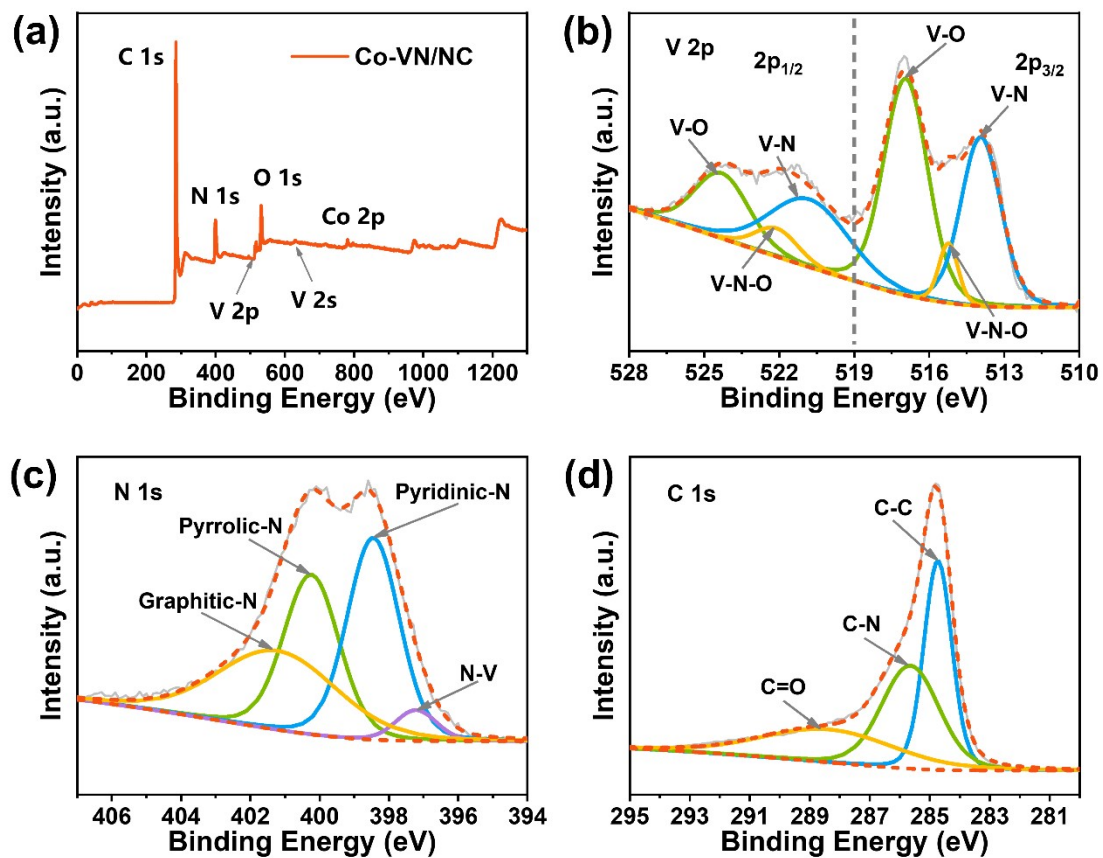


Figure S4. (a) XPS survey spectrum of Co-VN/NC. (b-d) High-resolution XPS spectra of V 2p, N 1s and C 1s in Co-VN/NC, respectively.

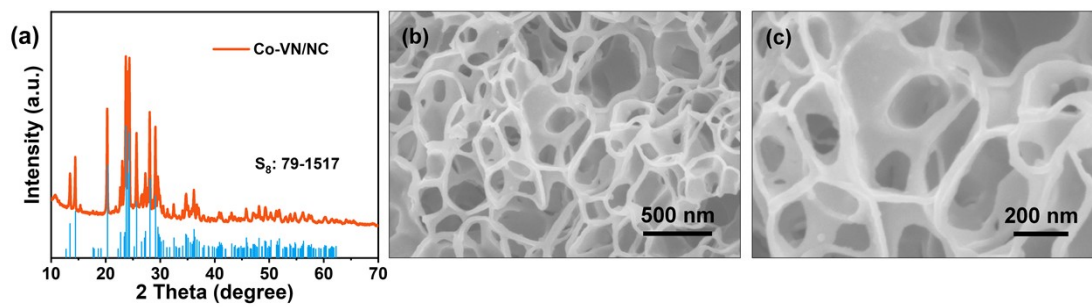


Figure S5. (a) XRD pattern of Co-VN/NC/S. (b, c) SEM images of Co-VN/NC/S at different magnifications.

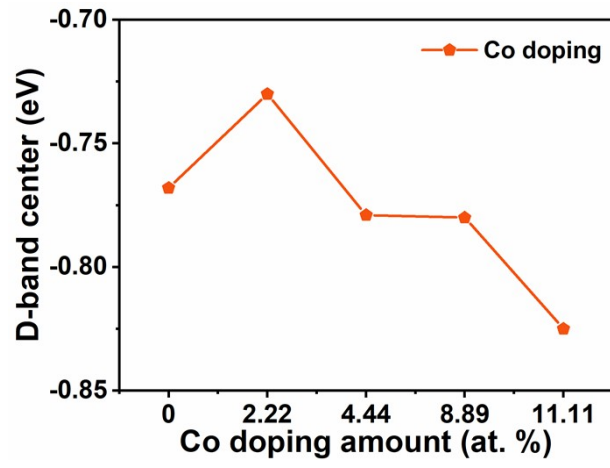


Figure S6. The d band center of Co-VN with different Co doping ratios.

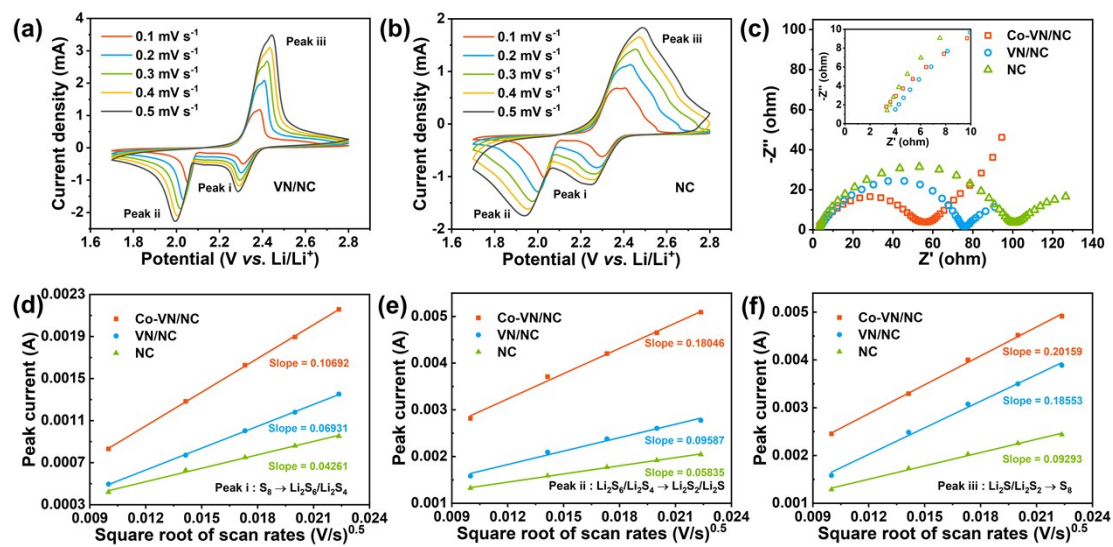


Figure S7. (a-b) CV curves of VN/NC and NC cathodes at different scan rates. (c) EIS curves were recorded for the three materials cathodes. (d-f) The corresponding linear fits of the peak currents to the square root of the scan rates.

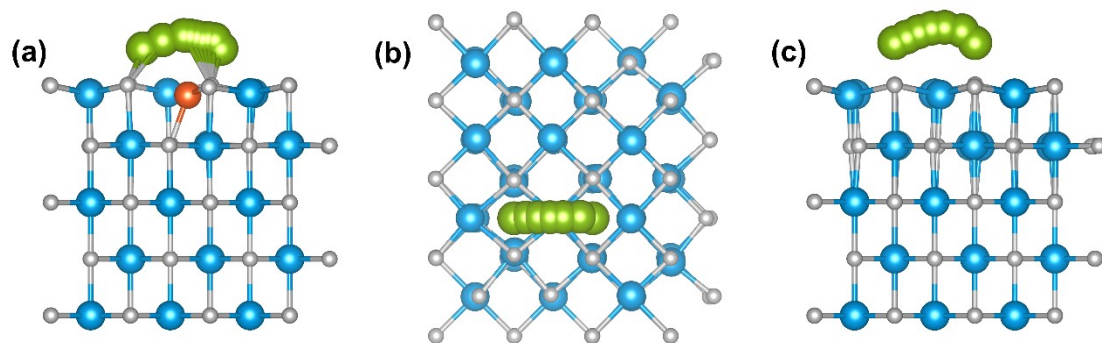


Figure S8. (a) Side view representations of Li-ion diffusion pathways on Co-VN (200) surfaces. (b-c) Top and side view representations of Li-ion diffusion pathways on VN (200) surfaces, respectively.

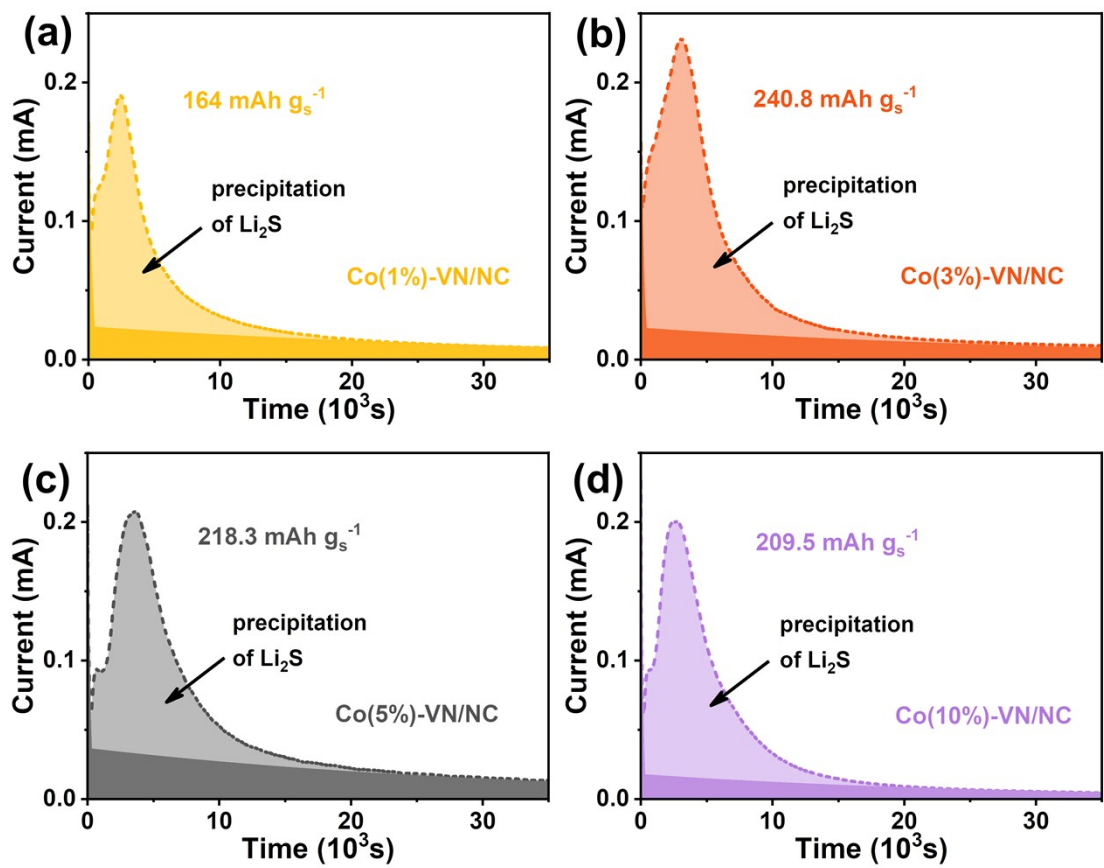


Figure S9. (a-d) Potentiostatic discharge curves of Co-VN/NC with different Co doping contents.

Table S1. The D_{ij} values were calculated at the peaks i, ii, iii of Co-VN/NC, VN/NC and NC cathodes.

CV Peak	Co-VN/NC	VN/NC	NC
Peak i	$1.632 \times 10^{-8} \text{ cm}^2/\text{s}$	$6.858 \times 10^{-9} \text{ cm}^2/\text{s}$	$2.592 \times 10^{-9} \text{ cm}^2/\text{s}$
Peak ii	$1.649 \times 10^{-8} \text{ cm}^2/\text{s}$	$1.312 \times 10^{-8} \text{ cm}^2/\text{s}$	$4.861 \times 10^{-9} \text{ cm}^2/\text{s}$
Peak iii	$5.802 \times 10^{-8} \text{ cm}^2/\text{s}$	$4.914 \times 10^{-8} \text{ cm}^2/\text{s}$	$1.233 \times 10^{-8} \text{ cm}^2/\text{s}$

Table S2. Compared performance of 3D Co-VN/NC and other similar studies reported in Li-S batteries.

Sulfur cathodes	Sulfur content (wt%)	Capacity at 2 C (mAh g ⁻¹)	High sulfur loading (mg cm ⁻²)	Areal capacity (mAh cm ⁻²)	References
Co-VN@C	70	650	3.61	3.5 at 0.2 C	[1]
Co-NbN/rGO	72	702	3.7	4.42 at 0.2 C	[2]
Co-VN microflowers	69.2	706	4.42	~3.86 at 0.2 C	[3]
VN@N-PGC	72	832	—	—	[4]
VN/NG	70	962	3.2	3.86 at 0.2 C	[5]
VN/N-rGO	78	872	4.1	3.22 at 1 C	[6]
Porous laminated VN	80	832.7	4.3	~5.16 at 0.2 C	[7]
VN@NG	70	830	7.3	~4.4 at 0.2 C	[8]
3D Co-VN/NC	79.8	868	4.83	4.98 at 0.2 C	This work

Supplementary References

1. W. J. Ren, L. Q. Xu, L. Zhu, X. Y. Wang, X. J. Ma and D. B. Wang, *ACS Appl. Mater. Interfaces*, 2018, **10**, 11642-11651.
2. W. N. Ge, L. Wang, C. C. Li, C. S. Wang, D. B. Wang, Y. T. Qian and L. Q. Xu, *J. Mater. Chem. A*, 2020, **8**, 6276-6282.
3. Z. Z. Cheng, Y. X. Wang, W. J. Zhang and M. Xu, *ACS Appl. Energy Mater.*, 2020, **3**, 4523-4530.
4. X. Y. Yang, S. Chen, W. B. Gong, X. D. Meng, J. P. Ma, J. Zhang, L. R. Zheng, H. D. Abruna and J. X. Geng, *Small*, 2020, **16**, 2004950.
5. E. D. Jing, L. Chen, S. D. Xu, W. Z. Tian, D. Zhang, N. N. Wang, Z. C. Bai, X. X. Zhou, S. B. Liu, D. H. Duan and X. Y. Qiu, *J. Energy Chem.*, 2022, **64**, 574-582.
6. J. Y. Xia, W. X. Hua, L. Wang, Y. F. Sun, C. N. Geng, C. Zhang, W. C. Wang, Y. Wan and Q.

- H. Yang, *Adv. Funct. Mater.*, 2021, **31**, 2101980.
7. R. Q. Liu, W. H. Liu, Y. L. Bu, W. W. Yang, C. Wang, C. Priest, Z. W. Liu, Y. Z. Wang, J. Y. Chen, Y. H. Wang, J. Cheng, X. J. Lin, X. M. Feng, G. Wu, Y. W. Ma and W. Huang, *ACS Nano*, 2020, **14**, 17308-17320.
 8. N. Li, Z. M. Xu, P. Wang, Z. A. Zhang, B. Hong, J. Li and Y. Q. Lai, *Chem. Eng. J.*, 2020, **398**, 125432.